Universality in ultradilute liquid Bose-Bose mixtures

V. Cikojević and L. Vranješ Markić*
Faculty of Science, University of Split, Ruđera Boškovića 33, HR-21000 Split, Croatia

G. E. Astrakharchik and J. Boronat
Departament de Física, Universitat Politècnica de Catalunya, Campus Nord B4-B5, E-08034 Barcelona, Spain

(Received 8 November 2018; published 13 February 2019)

We have studied dilute Bose-Bose mixtures of atoms with attractive interspecies and repulsive intraspecies interactions using quantum Monte Carlo methods at $T = 0$. Using a number of models for interactions, we determine the range of validity of the universal equation of state of the symmetric liquid mixture as a function of two parameters: the s-wave scattering length and the effective range of the interaction potential. It is shown that the Lee-Huang-Yang correction is sufficient only for extremely dilute liquids with the additional restriction that the range of the potential is small enough. Based on the quantum Monte Carlo equation of state we develop a density functional which goes beyond the Lee-Huang-Yang term and use it together with the local density approximation to determine density profiles of realistic self-bound drops.

DOI: 10.1103/PhysRevA.99.023618

I. INTRODUCTION

Dilute Bose and Fermi gases have proved to be a versatile tool for exploration of different phases of condensed-matter systems. For more than two decades, most of the experiments were done in the low-density gas phase, in the universal regime fixed solely by the gas parameter ρa^3, with a being the s-wave scattering length and ρ the density. The range of universality of the homogeneous Bose gas was established using different model potentials and solving the N-body problem in an exact way with quantum Monte Carlo methods [1]. One of the most important advances in the field of ultracold atoms in the past years is the recent creation of ultradilute quantum droplets. Such self-bound quantum systems were first experimentally observed for dipolar atoms [2–4] being caused by a close cancellation of the dipolar and short-range energies. Petrov [5] pointed out that liquid drops can be created in an even simpler setup composed by a two-component mixture of bosons with short-ranged attractive interspecies and repulsive intraspecies interactions. However, the perturbative technique employed by Petrov is valid only very close to the mean-field (MF) instability limit, that is, for extremely dilute liquids. The collapse predicted on the MF level is avoided by stabilization due to the quantum fluctuations described by the Lee-Huang-Yang (LHY) correction to the energy. It was shown that a similar stabilization mechanism can be used in two- and one-dimensional geometries where the resulting liquid phase has enhanced stability [6]. Very recently, two experimental groups managed to obtain self-bound liquid drops [7,8] which, upon releasing the trap, did not expand. The drops required a certain critical number of atoms to be bound. Importantly, measurements of the critical number and size of the smallest droplets could not be fully accounted for by the MF + LHY term [7].

Recently, some of us have studied liquid Bose-Bose droplets by using the diffusion Monte Carlo (DMC) method, thus solving *exactly* the full many-body problem for a given Hamiltonian at zero temperature [9]. Our results have confirmed the transition from a gas, with positive energy, to a self-bound droplet with negative energy. Furthermore, we have determined the critical number of atoms needed to form a liquid droplet as a function of the intraspecies scattering length. Using two different models for the attractive interaction, we did not get quantitatively the same results for the range of scattering lengths studied, which points to the lack of universality in terms of ρa^3. It is thus of fundamental interest to find whether there is a range of densities and scattering lengths where such universality exists. This is in fact expected when the system is very close to the MF collapse. In the case of homogeneous Bose gases, departures from universality start to appear around $\rho a^3 \gtrsim 10^{-3}$ [1]. In that case, adding the LHY correction allowed for a good approximation of the equation of state up to higher densities. Recently, a variational hypernetted-chain Euler-Lagrange calculation [10] of unbalanced mixtures showed that the drops can only be stable in a very narrow range, near an optimal ratio of partial densities and near the energy minimum. Moreover, Ref. [10] found dependence on the effective range even at low densities.

In this article, we use the DMC method to address the question of the universality in the equation of state of dilute Bose-Bose mixtures. The second question we pose here is whether there exists a regime where instead of using only one parameter (s-wave scattering length) inclusion of an additional parameter (effective range [11]) extends the validity of the universal description. To answer these questions directly for finite-size droplets would require enormous computational resources, as at least thousands of atoms are needed to achieve a self-bound state close to the mean-field limit [7]. In order to eliminate the finite-size effects caused by the surface tension and simplify the analysis, we study here bulk properties corresponding to the interior of large saturated droplets. From the obtained equation of state we construct a new density

*Corresponding author: leandra@pmfst.hr

functional and use it to predict the profiles of the drops, discussing the effects of the potential range.

II. METHODS

We rely on the DMC method, which was successfully used in the past for determining the ground-state properties of interacting many-body systems. The DMC method stochastically solves the imaginary-time Schrödinger equation, giving for bosonic systems exact results within the statistical noise [12]. The Hamiltonian of our system is given by

$$H = -\sum_{\alpha=1}^{2} \frac{\hbar^2}{2m_\alpha} \sum_{i=1}^{N_\alpha} \nabla_{i\alpha}^2 + \frac{1}{2} \sum_{\alpha,\beta=1}^{2} \sum_{i_\alpha, j_\beta=1}^{N_\alpha, N_\beta} V^{(\alpha,\beta)}\left(r_{i_\alpha j_\beta}\right), \quad (1)$$

where $V^{(\alpha,\beta)}(r)$ is the interatomic interaction between species α and β. The intraspecies interactions with positive s-wave scattering length are modeled either by a hard-core potential of diameter a_{ii} or by a 10-6 potential [13] that does not support a two-body bound state, $V(r) = V_0[(\frac{r_0}{r})^{10} - (\frac{r_0}{r})^6]$.

The latter model has an analytic scattering length given in Ref. [13]. The interspecies interactions with negative scattering length, $a_{12} < 0$, are modeled by a square-well potential of range R and depth $-V_0$ or by a 10-6 potential with no bound states.

We resort to a second-order DMC method and use a guiding wave function to reduce the variance, as described in Ref. [12]. We construct the trial wave function as a product of Jastrow factors [14]:

$$\Psi(\mathbf{R}) = \prod_{1=i<j}^{N_1} f^{(1,1)}(r_{ij}) \prod_{1=i<j}^{N_2} f^{(2,2)}(r_{ij}) \prod_{i,j=1}^{N_1,N_2} f^{(1,2)}(r_{ij}). \quad (2)$$

The particular form of the two-particle correlation function depends on the model of the interaction potential. For the hard-core potential we use

$$f^{\alpha,\alpha}(r) = \begin{cases} 1 - a_{\alpha,\alpha}/r, & r < \tilde{R}, \\ B\exp\left(-\frac{C}{r} + \frac{D}{r^2}\right), & \tilde{R} < r < L/2, \\ 1, & r > L/2, \end{cases} \quad (3)$$

The parameter $\tilde{R}$ can be optimized, but energies do not change drastically when $\tilde{R} \approx L/2$; so we set $\tilde{R} = 0.9L/2$. Other parameters are obtained by continuity conditions for the function and its first derivative. For the square-well potential we use

$$f^{\alpha,\beta}(r) = \begin{cases} \sin(kr)/r, & r < R, \\ A(1 - \tilde{a}_{\alpha,\beta}/r), & R < r < \tilde{R}, \\ B\exp\left(-\frac{C}{r} + \frac{D}{r^2}\right), & \tilde{R} < r < L/2, \\ 1, & r > L/2, \end{cases} \quad (4)$$

where $\tilde{a}_{\alpha,\beta}$ is a variational parameter. We set $\tilde{R} = 0.9L/2$, while other parameters are obtained by continuity conditions. Finally, for the 10-6 potential we use

$$f^{\alpha,\beta}(r) = \begin{cases} h(r, \tilde{a}_{\alpha,\beta}), & r < R_0, \\ B\exp\left(-\frac{C}{r} + \frac{D}{r^2}\right), & R_0 < r < L/2, \\ 1, & r > L/2, \end{cases} \quad (5)$$

where $h(r, \tilde{a}_{\alpha,\beta})$ is the two-body scattering solution given in Ref. [13]. This function has a variational parameter $\tilde{a}_{\alpha,\beta}$, and we set $R_0 = 0.9L/2$. Zero derivative is imposed at the half size of the simulation box L for all three Jastrow factors.

We consider a mixture with equal masses of particles $m_1 = m_2 = m$. Such a situation is typical in experiments where different hyperfine states of the same atomic species are used to create two components [7]. Furthermore, in order to reduce the number of degrees of freedom we choose to study the symmetric mixture with $a_{11} = a_{22}$ resulting in $N_1 = N_2$. The calculations are performed in a box with periodic boundary conditions.

To approach the thermodynamic limit, we investigate finite-size effects by increasing the number of particles up to the point where energy converges. DMC results are presented for the largest particle number used. In Fig. 1, we show the convergence for three different a_{12}/a_{11} values. It is possible to obtain the finite-size correction analytically only very close to the mean-field instability limit. In that case, the leading correction to the mean-field (Hartree) contribution comes from the intracomponent number of pairs $N_1(N_1 - 1)/2$,

$$\frac{\Delta E_{\mathrm{MF}}(N)}{N} = -\frac{\pi}{6} \frac{\hbar^2}{m a_{11}^2} \frac{2\pi}{N} \rho a_{11}^3, \quad (6)$$

where $N = 2N_1$. This correction is negative, linear with the density, and decreases as N^{-1} with the number of particles. This correction is also shown in Fig. 1.

We also optimize the time-step and population bias to reduce their influence below the statistical noise.

III. RESULTS

First, we report results obtained using the hard-core model for the repulsive interactions and a square-well (SW) potential for the attractive ones. In Fig. 2, we show our results for different values of the interspecies scattering length a_{12} and different ranges of the attractive well R, and we compare them to the MF + LHY prediction [5]. The equation of state in Ref. [5] for $m_2 = m_1 = m$, $a_{22} = a_{11}$, and $N_2 = N_1$ is given by

$$\frac{E}{N} = \frac{\hbar^2 \pi (a_{11} + a_{12})}{m} \rho + \frac{32\sqrt{2\pi}}{15} \frac{\hbar^2 a_{11}^{5/2}}{m} f\left(\frac{a_{12}^2}{a_{11}^2}\right) \rho^{3/2}, \quad (7)$$

with $f(x) = (1 + \sqrt{x})^{5/2} + (1 - \sqrt{x})^{5/2}$.

Notice that the function $f(x)$ becomes complex for $a_{12} < -a_{11}$ and the presence of the imaginary component reduces the applicability of the perturbative theory. If instead the argument is approximated by $x = a_{12}^2/a_{11}^2 = 1$ so that the function $f(x)$ remains real, as it was done in Ref. [5], Eq. (7) reduces to the following form,

$$\frac{E}{N} = \frac{\hbar^2 \pi (a_{11} + a_{12})}{m} \rho + \frac{256\sqrt{\pi}}{15} \frac{\hbar^2 a_{11}^{5/2}}{m} \rho^{3/2}, \quad (8)$$

shown with a dashed line in Fig. 2. We plot as well the energy resulting from taking the real part of $f(x)$ (7), without invoking the approximation $x = 1$. Only very close to the $a_{12} = -a_{11}$ limit corresponding to zero equilibrium density, both predictions are nearly the same while they clearly differ for finite densities. We report the exact DMC energies in Fig. 2. The perturbative MF + LHY results are recovered for small range R of the square well and $\rho a_{11}^3 \approx 10^{-6}$ [see Fig. 2(a)]. However, when R is increased by a large amount

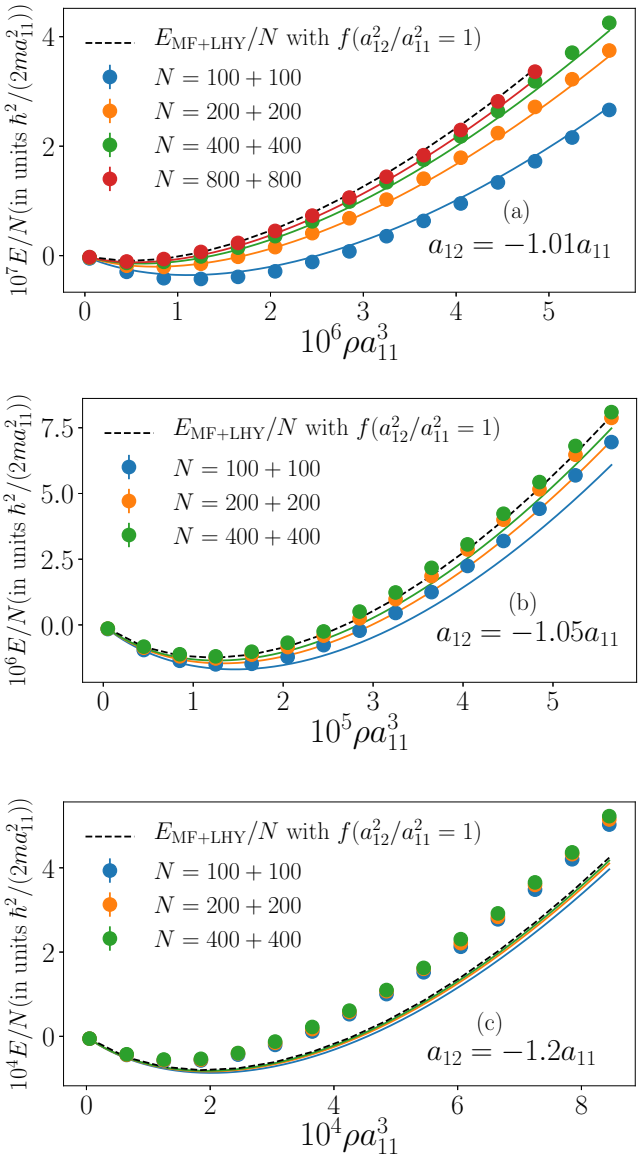

FIG. 1. The energy per particle as a function of the density for $a_{12}=-1.01a_{11}$, $-1.05a_{11}$, and $-1.2a_{11}$. Different total number of particles N is used to illustrate the finite-size effect. Results are obtained with the hard-core model of diameter a_{11} for the repulsive intraspecies interaction and a square-well potential with diameter $\rho R^3=10^{-5}$ for interspecies attraction. Solid lines are finite-size corrections coming from the mean-field energy Eq. (6) and the dashed line is the MF + LHY result.

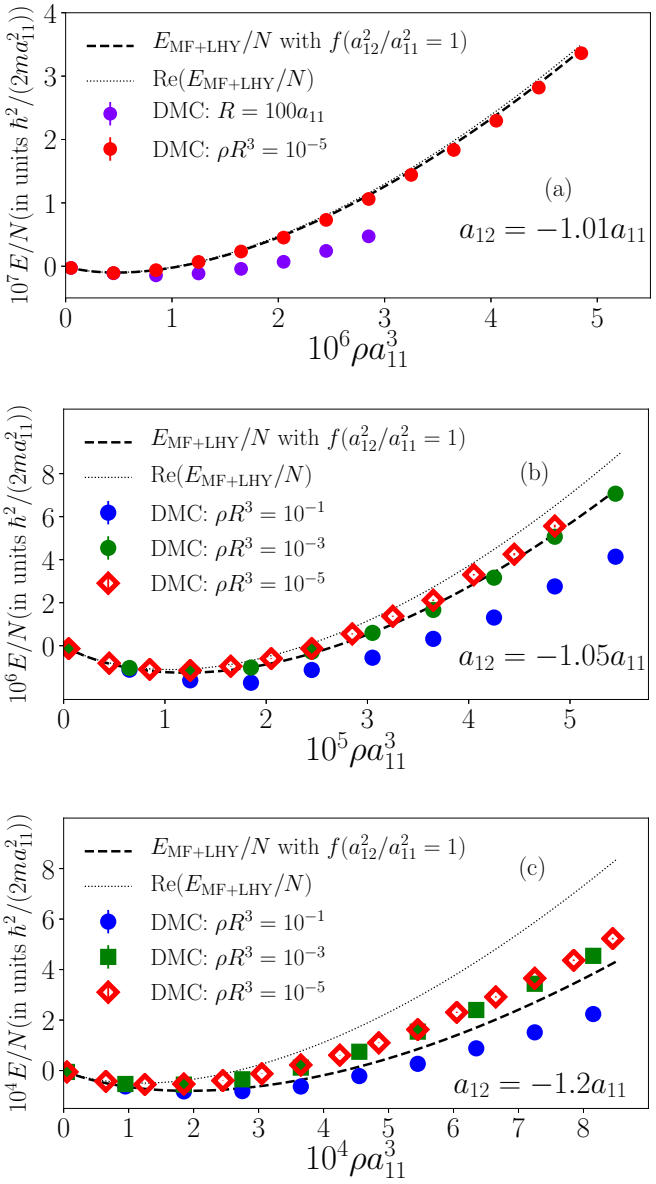

FIG. 2. DMC equation of state of the liquid mixture for different values of a_{12} and different ranges R, in comparison with MF + LHY theory.

(to $R=100a_{11}$) the universality breaks at $\rho R^3\simeq 10^{-1}$. The energies for experimentally relevant densities, $\rho a_{11}^3\approx 10^{-5}$ [7,8], are reported in Fig. 2(b). In this case and for larger densities [Fig. 2(c)], we observe that the energy depends on the potential range. Furthermore, the two ways of writing the perturbative equation of state, given by Eqs. (7) and (8), differ among themselves but are not equal to the obtained DMC equation of state. The latter appears to be independent of R up to approximately $\rho R^3=10^{-3}$. Indeed, the difference between the energy per particle E/N calculated at $\rho R^3=10^{-3}$ and $\rho R^3=10^{-5}$ is at most 3 error bars, or 6% at the highest density and at most 4% in the minimum.

It can be noted that within perturbative theory the energy is a single curve written in units of the equilibrium energy E_0 and density ρ_0. That is, the equation of state (8) can be conveniently represented as a $(E/E_0,\rho/\rho_0)$ curve,

$$\frac{E}{|E_0|}=-3\left(\frac{\rho}{\rho_0}\right)+2\left(\frac{\rho}{\rho_0}\right)^{3/2}, \tag{9}$$

with, for the symmetric mixture, $\rho_0=25\pi(a_{11}+a_{12})^2/(16384a_{11}^5)$ and $E_0/N=-25\pi^2\hbar^2|a_{11}+a_{12}|^3/(49152ma_{11}^5)$.

The DMC equations of state for different scattering lengths are shown in Fig. 3. The results are obtained for a sufficiently small potential range, $\rho R^3=10^{-5}$, ensuring the universality in terms of the s-wave scattering length. As already observed in Fig. 2, when $|a_{12}|\approx a_{11}$, the MF + LHY prediction is recovered. By increasing $|a_{12}|/a_{11}$, we find repulsive

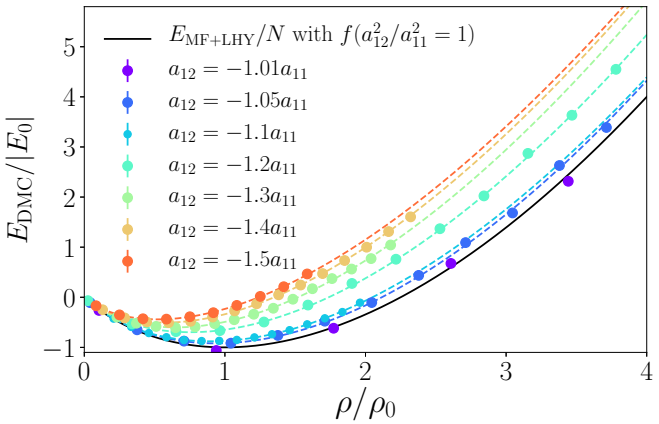

FIG. 3. Equations of state for different a_{12}/a_{11} normalized to the density and the energy at the MF + LHY equilibrium point (ρ_0, E_0). Dashed lines show fits to the data in the form of $E/N = \alpha x + \beta x^\gamma$, with $x = \rho a_{11}^3$. The range of the square well is $\rho R^3 = 10^{-5}$.

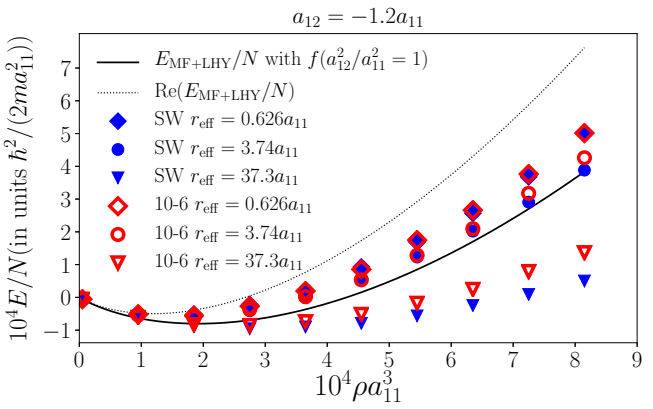

FIG. 4. Dependence of the equation of state on the effective range.

contributions to the energy beyond the LHY terms. At the same time, the equilibrium densities become lower compared to the ones predicted by Eq. (9), which was obtained by calculating the $f(x)$ function at $x = 1$. If instead one uses Eq. (7) derived by taking the real part of $f(x)$, weaker binding is predicted as compared to DMC results. Thus, as we can see in Fig. 2, for small ranges $\rho R^3 = 10^{-5}$, the DMC many-body prediction is between Eqs. (7) and (9), but closer to Eq. (9). The DMC values of the equilibrium energies and densities are reported in Table I. They are also compared to predictions from perturbative theory given by Eq. (9). With the increase of $|a_{12}|/a_{11}$ the equilibrium and spinodal densities start to depart significantly from the MF + LHY values. It is worth noticing again that the MF + LHY equation of state becomes complex, and thus unphysical, unless the approximation $f(a_{12}^2/a_{11}^2 = 1)$ is used. Our results show that even very small (in absolute value) negative pressures can cause spinodal instability. For typical experimental parameters $a_{11} = 50a_0$ [7,8] the uniform liquid breaks into droplets when the applied negative pressure is very small, from 1.81 pPa for $a_{12} = -1.05a_{11}$ to 31.3 nPa for $a_{12} = -1.5a_{11}$.

TABLE I. Energies (equilibrium and spinodal) and densities for different scattering lengths a_{12}/a_{11} for small ranges $\rho R^3 = 10^{-5}$. Here the subscript "eq" stands for the minimum from the fit to DMC energy shown in Fig. 3, the subscript "0" stands for the minimum of the perturbative equation of state given by Eq. (9), and the spinodal point is denoted by the subscript "sp" from the fit on DMC data and the subscript "sp,0" in the case of Eq. (9).

$\frac{a_{12}}{a_{11}}$	$\frac{10^5\rho_{\rm eq}}{a_{11}^{-3}}$	$\frac{\rho_{\rm eq}}{\rho_0}$	$\frac{10^5\rho_{\rm sp}}{a_{11}^{-3}}$	$\frac{\rho_{\rm sp}}{\rho_{\rm sp,0}}$	$\frac{10^6\hbar^2E_{\rm eq}}{2ma_{11}^2N}$	$\frac{E_{\rm eq}}{E_0}$
−1.05	1.12	0.934	0.715	0.932	−1.15	0.919
−1.10	4.28	0.894	2.73	0.888	−8.82	0.879
−1.20	14.5	0.754	9.19	0.749	−56.0	0.697
−1.30	28.0	0.649	17.7	0.641	−163	0.601
−1.40	44.9	0.585	28.3	0.576	−334	0.520
−1.50	62.4	0.521	39.3	0.512	−554	0.441

As can be seen from Fig. 2, the equation of state loses universality in terms of the scattering length when $\rho R^3 \gtrsim 10^{-3}$. This poses the relevant question of whether by fixing one more parameter, besides the s-wave scattering length, it is possible to obtain a universal description.

To address this question, we perform DMC calculations using the 10-6 model with equivalent values of the s-wave scattering lengths and the effective range $r_{\rm eff}$ of the attractive interaction. For the repulsive interactions, we fix the range of the 10-6 model potential to $r_0 = 2a_{11}$. In Fig. 4, we show results for the scattering length $a_{12} = -1.2a_{11}$ and three values of the effective range $r_{\rm eff}$. The solid line is for Eq. (8) and the dashed one is for the real part of Eq. (7). The range of the SW potential is $R/a_{11} = 0.531$, 2.17, and 9.18 when $r_{\rm eff}/a_{11} = 0.626$, 3.74, and 37.3, respectively. We find that, specifying only the scattering length, one cannot generally obtain universal results unless the range is sufficiently small, $\rho R^3 \lesssim 10^{-1}$. The interaction potential for a given scattering length predicts different energies and equilibrium densities when different effective ranges are used. Generally, increasing the range lowers the energy and shifts the equilibrium density to larger values. However, if we specify both the scattering length and the effective range, then we observe that the difference between the results of two models is always smaller than the difference between the results for the same type of model but with different ranges. In Fig. 4, the two models with $r_{\rm eff}/a_{11} = 0.626$ give, within error bars, the same energies in the whole density range. Increasing the range, at higher densities we observe that the two potentials start to give different predictions and that the difference between them grows with the increase in density. Interestingly, even when the effective range is quite large, $r_{\rm eff}/a_{11} = 37.3$, the relative difference between the models remains lower than 10%, as long as $\rho R^3 < 0.2$. Increasing the density even further, we would need more parameters beyond a_{12} and $r_{\rm eff}$ to describe the interaction.

The observed dependence on the effective range for $\rho_{\rm eq} R^3 > 10^{-3}$ is in overall agreement with recent calculations of unbalanced mixtures [10] based on the variational hypernetted chain method. It is interesting to notice that the MF + LHY equations of state, following Eq. (9), are actually closer to our full many-body calculations using rather large values of the effective range. On the other hand, the results

using only the real part of Eq. (7) are above the DMC energies for even the smallest range.

Presuming that the equation of state of the liquid mixture is universal in terms of the scattering length and the effective range for $\rho R^3 \lesssim 10^{-1}$, we use the SW results to deduce the following form for the equation of state,

$$\frac{E}{N} = \frac{|E_0|}{N}\left[-3\left(\frac{\rho}{\rho_0}\right) + \beta\left(\frac{\rho}{\rho_0}\right)^{\gamma}\right], \tag{10}$$

where β and γ are functions of a_{12}/a_{11} and $r_{\rm eff}/a_{11}$:

$$\beta = \beta_{01}\frac{a_{12}}{a_{11}} + \left(\beta_{10} + \beta_{11}\frac{a_{12}}{a_{11}}\right)\frac{R(a_{12}, r_{\rm eff})}{a_{11}}, \tag{11}$$

$$\gamma = \gamma_{00} + \gamma_{01}\frac{a_{12}}{a_{11}} + \left(\gamma_{10} + \gamma_{11}\frac{a_{12}}{a_{11}}\right)\frac{R(a_{12}, r_{\rm eff})}{a_{11}}. \tag{12}$$

R is the square-well diameter associated with the given a_{12} and $r_{\rm eff} > 0$. It can be calculated numerically for given a_{12} and $r_{\rm eff}$, and we provide a numerical code in Ref. [15]. There are 7 free parameters in the model: β_{01}, β_{10}, β_{11}, γ_{00}, γ_{01}, γ_{10}, and γ_{11}. They are obtained by fitting 18 equations of state with different R and a_{12}. In particular, the chosen a_{12}/a_{11} values were -1.01, -1.05, -1.08, -1.1, and -1.2. The obtained values of the parameters are given in Table II.

With these values, $\beta(a_{12} = -a_{11}, R = 0) = 1.956 \pm 0.003$ and $\gamma(a_{12} = -a_{11}, R = 0) = 1.51 \pm 0.02$, which is very close to the MF + LHY values: $\beta = 2$ and $\gamma = 1.5$. We then verify that this form predicts well the equation of state up to $a_{12} = -1.3a_{11}$ provided that R is not too large ($\rho R^3 < 10^{-1}$).

TABLE II. Parameters of the equation of state.

β_{01}	β_{10}	β_{11}	γ_{00}	γ_{01}	γ_{10}	γ_{11}
−1.956(3)	0.231(5)	0.236(5)	1.83(2)	0.32(2)	0.030(3)	0.030(3)

The equation of state (10) can be used as an energy functional [16] to calculate density profiles of liquid mixture drops within the local-density approximation (LDA). Starting from the DMC equation of state and using LDA we obtain density profiles of drops for different scattering lengths and effective ranges and compare them with MF+LHY predictions in Fig. 5. To do so we write the energy functional as

$$\mathcal{E} = \frac{\hbar^2}{2m}N|\nabla\phi|^2 + \frac{25\pi^2\hbar^2|a_{11} + a_{12}|^3}{49152ma_{11}^5} \times\left[-3\frac{N^2|\phi|^4}{\rho_0} + \beta\frac{(N|\phi|^2)^{\gamma+1}}{\rho_0^{\gamma}}\right],$$

where N is the number of particles and ϕ is normalized as $\int d^3r|\phi|^2 = 1$. Then, we find the stationary solution of the

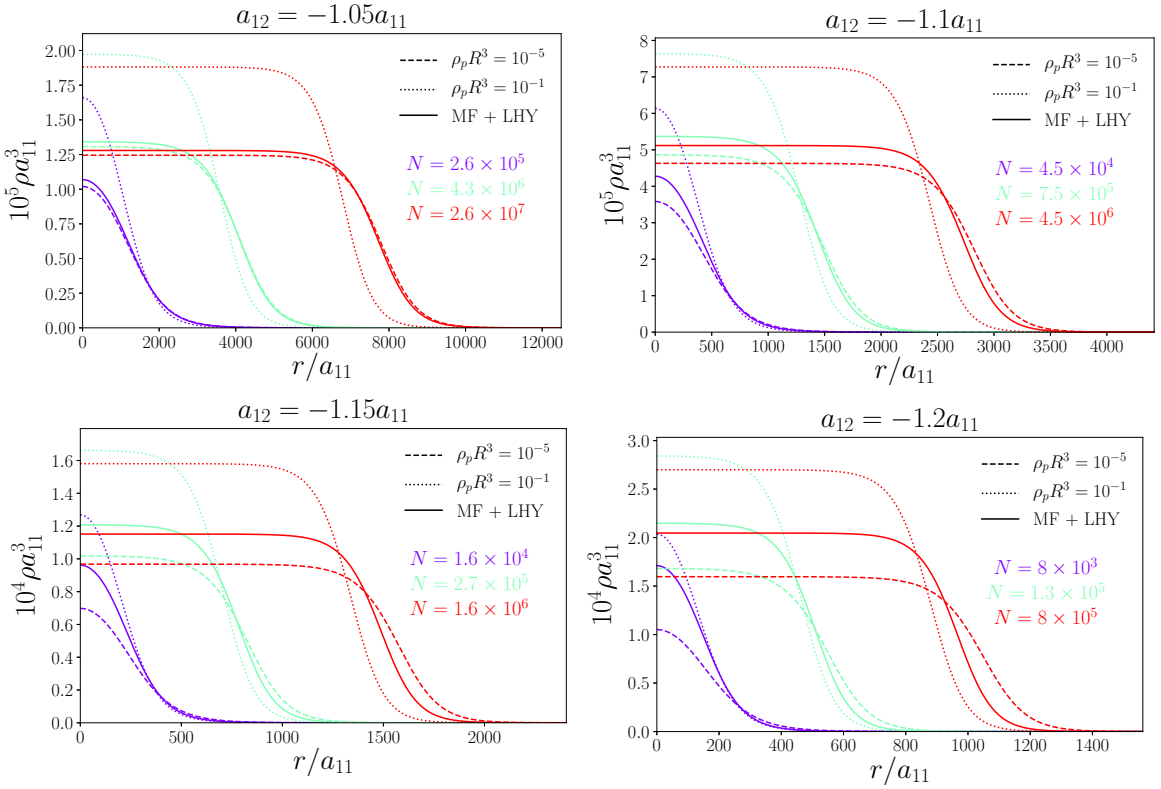

FIG. 5. Density profiles of drops with different scattering lengths and ranges compared to MF + LHY predictions. Dashed and dotted lines correspond to LDA calculations using the energy functional (Eq. 10) for $\rho_p R^3 = 10^{-5}$ (dashed line) and $\rho_p R^3 = 10^{-1}$ (dotted line), where $\rho_p = 25\pi(a_{11} + a_{12})^2/(16384a_{11}^5)$ is the equilibrium density from the MF + LHY theory. Solid lines correspond to MF + LHY calculations using the approximation $f(a_{12}^2/a_{11}^2 = 1)$. For each a_{12} and R, we show profiles for three different values of particle numbers, written below the legend, distinguished by color and growing from purple to red. Profiles with the smallest particle numbers (purple color) are stable ($E < 0$) and close to the critical number $N_c = 22.55 \times 96\sqrt{6}/(5\pi^2|1 + a_{12}/a_{11}|^{5/2})$ [5].

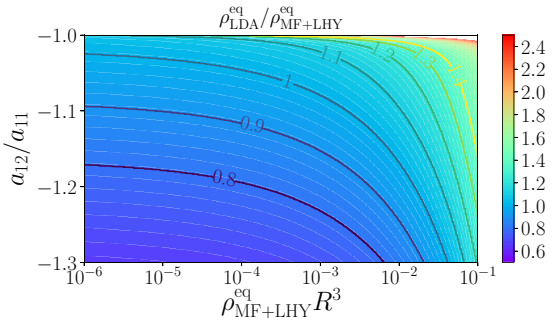

FIG. 6. Ratio of equilibrium densities $\rho^{eq}_{LDA}/\rho^{eq}_{MF+LHY}$ vs scattering length a_{12} and the range R. Isolines follow values with the constant $\rho^{eq}_{LDA}/\rho^{eq}_{MF+LHY}$. LDA results are obtained starting from the DMC equation of state.

equation of motion

$$i\hbar\frac{\partial\phi}{\partial t} = -\frac{\hbar^2\nabla^2\phi}{2m} + \frac{25\pi^2\hbar^2|a_{11}+a_{12}|^3}{49152ma_{11}^5} \times\left[-6\frac{N|\phi|^2}{\rho_0}+\beta(1+\gamma)\left(\frac{N|\phi|^2}{\rho_0}\right)^{\gamma}\right]\phi$$

by propagating it in imaginary time. The results for the equilibrium density as a function of the interspecies scattering length and the square-well range are presented in Fig. 6 and compared to the MF + LHY predictions. For a negligible range R, the equilibrium density drops below the MF + LHY prediction as $|a_{12}|/a_{11}$ is increased. The effect of the finite range is to increase the equilibrium density. That is by increasing R, the LDA prediction crosses the perturbative result of MF + LHY and goes above. Overall, by increasing the range and decreasing $|a_{12}|/a_{11}$ (i.e., going in the upright direction in Fig. 6) we observe an increase of $\rho^{eq}_{LDA}/\rho^{eq}_{MF+LHY}$.

IV. SUMMARY AND CONCLUSION

We have carried out high-precision DMC calculations of the ground-state equation of state of ultradilute two-component Bose liquids. We have found that the use of only the first beyond-MF correction, the LHY term, is accurate only for extremely small densities and only when the range of the interaction is not very large. In our study, we have used for the range R the diameter of the square-well potential, which has the same scattering length and effective range as the chosen model. If $|a_{12}/a_{11}+1|\leqslant 0.05$ and $\rho R^3 < 10^{-3}$, one parameter, the s-wave scattering length, is enough to describe the system, but there is an appreciable difference with respect to MF + LHY. Increasing the range, one enters a regime where interaction potentials with the same scattering length and effective range give equivalent results within 10%, which means that up to $\rho R^3 = 0.1$ we have at hand a universal equation of state which is a function of two parameters. For even larger values of ρR^3 additional parameters would need to be specified. The results of scattering calculations of alkali-metal atoms, such as given in Refs. [17,18], indicate that most likely the effective ranges are quite far from the zero-range limit. In that case, to obtain the correct results one needs a full many-body approach like DMC. Here, we provide an energy functional based on the best fit to DMC data and use it to calculate the density profiles of realistic drops with the LDA.

ACKNOWLEDGMENTS

We acknowledge fruitful discussions with Leticia Tarruell. This work has been supported in part by the Croatian Science Foundation under Project No. IP-2014-09-2452. Partial financial support from the MINECO (Spain) under Grants No. FIS 2014-56257-C2-1-P and No. FIS2017-84114-C2-1-P is also acknowledged. The computational resources of the Isabella Cluster at Zagreb University Computing Center (Srce) and Croatian National Grid Infrastructure (CRO NGI) were used. The Barcelona Supercomputing Center (The Spanish National Supercomputing Center, Centro Nacional de Supercomputación) is acknowledged for providing computational facilities (Grant No. RES-FI-2018-3-0027).

[1] S. Giorgini, J. Boronat, and J. Casulleras, Phys. Rev. A **60**, 5129 (1999).
[2] H. Kadau, M. Schmitt, M. Wenzel, C. Wink, T. Maier, I. Ferrier-Barbut, and T. Pfau, Nature (London) **530**, 194 (2016).
[3] I. Ferrier-Barbut, H. Kadau, M. Schmitt, M. Wenzel, and T. Pfau, Phys. Rev. Lett. **116**, 215301 (2016).
[4] M. Schmitt, M. Wenzel, F. Böttcher, I. Ferrier-Barbut, and T. Pfau, Nature (London) **539**, 259 (2016).
[5] D. S. Petrov, Phys. Rev. Lett. **115**, 155302 (2015).
[6] D. S. Petrov and G. E. Astrakharchik, Phys. Rev. Lett. **117**, 100401 (2016).
[7] C. Cabrera, L. Tanzi, J. Sanz, B. Naylor, P. Thomas, P. Cheiney, and L. Tarruell, Science **359**, 301 (2018).
[8] G. Semeghini, G. Ferioli, L. Masi, C. Mazzinghi, L. Wolswijk, F. Minardi, M. Modugno, G. Modugno, M. Inguscio, and M. Fattori, Phys. Rev. Lett. **120**, 235301 (2018).
[9] V. Cikojević, K. Dželalija, P. Stipanović, L. Vranješ Markić, and J. Boronat, Phys. Rev. B **97**, 140502 (2018).
[10] C. Staudinger, F. Mazzanti, and R. E. Zillich, Phys. Rev. A **98**, 023633 (2018).
[11] R. G. Newton, *Scattering Theory of Waves and Particles* (Springer-Verlag, New York, 1982); P. Roman, *Advanced Quantum Theory* (Addison-Wesley, Reading, MA, 1965).
[12] J. Boronat and J. Casulleras, Phys. Rev. B **49**, 8920 (1994).
[13] J. Pade, Eur. Phys. J. D **44**, 345 (2007).
[14] L. Reatto and G. V. Chester, Phys. Rev. **155**, 88 (1967).
[15] https://github.com/viktorcikojevic/Square-well-range-R-a12-reff-/tree/master.
[16] F. Ancilotto, M. Barranco, M. Guilleumas, and M. Pi, Phys. Rev. A **98**, 053623 (2018).
[17] V. V. Flambaum, G. F. Gribakin, and C. Harabati, Phys. Rev. A **59**, 1998 (1999).
[18] L. Tanzi, C. R. Cabrera, J. Sanz, P. Cheiney, M. Tomza, and L. Tarruell, Phys. Rev. A **98**, 062712 (2018).